HYDROLOGICAL PROCESSES
Hydrol. Process. **29**, 3954–3965 (2015)
Published online 14 July 2015 in Wiley Online Library
(wileyonlinelibrary.com) DOI: 10.1002/hyp.10573

A radiative–conductive–convective approach to calculate thaw season ground surface temperatures for modelling frost table dynamics

Tyler J. Williams,[1,2]* John W. Pomeroy,[1] J Richard Janowicz,[2] Sean K. Carey,[3] Kabir Rasouli[1] and William L. Quinton[4]

[1] *Centre for Hydrology, University of Saskatchewan, Saskatoon, SK, Canada*
[2] *Water Resources Branch, Yukon Environment, Whitehorse, YT, Canada*
[3] *School of Geography & Earth Sciences, McMaster University, Hamilton, ON, Canada*
[4] *Cold Regions Research Centre, Wilfrid Laurier University, Waterloo, ON, Canada*

Abstract:

The frost table depth is a critical state variable for hydrological modelling in cold regions as frozen ground controls runoff generation, subsurface water storage and the permafrost regime. Calculation of the frost table depth is typically performed using a modified version of the Stefan equation, which is driven with the ground surface temperature. Ground surface temperatures have usually been estimated as linear functions of air temperature, referred to as '*n*-factors' in permafrost studies. However, these linear functions perform poorly early in the thaw season and vary widely with slope, aspect and vegetation cover, requiring site-specific calibration. In order to improve estimation of the ground surface temperature and avoid site-specific calibration, an empirical radiative–conductive–convective (RCC) approach is proposed that uses air temperature, net radiation and antecedent frost table position as driving variables. The RCC algorithm was developed from forested and open sites on the eastern slope of the Coastal Mountains in southern Yukon, Canada, and tested at a high-altitude site in the Canadian Rockies, and a peatland in the southern Northwest Territories. The RCC approach performed well in a variety of land types without any local calibration and particularly improved estimation of ground temperature compared with linear functions during the first month of the thaw season, with mean absolute errors $<2\,^{\circ}C$ in seven of the nine sites tested. An example of the RCC approach coupled with a modified Stefan thaw equation suggests a capability to represent frozen ground conditions that can be incorporated into hydrological and permafrost models of cold regions. Copyright © 2015 John Wiley & Sons, Ltd.

KEY WORDS frozen soil; ground thaw; active layer; permafrost; cold regions hydrology; *n*-factor; hydrological modelling

Received 18 November 2014; Accepted 5 June 2015

INTRODUCTION

A distinct feature of modelling cold region hydrological processes is the need to represent frozen soils that exert a large impact on the soil energy balance and hydraulic properties. As soil moisture content increases, the frozen soil becomes increasingly impenetrable to infiltrating water (Woo, 1986). The position of the frost table (approximately the zero-degree isotherm during soil thawing) relative to the ground surface thus limits the depth at which subsurface flow occurs. Because the hydraulic conductivity of organic soils decreases by several orders of magnitude with depth (Quinton *et al.*, 2009), the position of the frost table has the potential to strongly control the rate and direction of subsurface flow.

Simulating ground thaw depth for the purpose of incorporating it into large scale hydrological models requires a balance between process accuracy and simplicity of data requirements. A wide range of empirical, semi-empirical, analytical and numerical equations have been used to calculate progression of the thawing front as summarized by Zhang *et al.* (2008). One of the most common techniques utilized in the literature is a modified Stefan equation (Zhang *et al.*, 2000; Woo *et al.*, 2004; Carey and Woo, 2005; Hayashi *et al.*, 2007). A limitation with this approach is the requirement for a reference ground surface temperature as the upper-boundary condition, which is the temperature at the top of the soil, organic layer or bedrock ground surface. Unfortunately this reference temperature for soil-heat conduction is not necessarily

*Correspondence to: Tyler J. Williams, Water Resources Branch, Yukon Environment, Whitehorse, Yukon.
E-mail: tjw2@alumni.sfu.ca

the surface temperature that is the common reference for radiative and turbulent transfer to the atmosphere, as that temperature is often the temperature at the top of the plant canopy, organic debris or snow surface and is not always well related to underlying upper soil temperatures. As such, the upper-boundary ground surface temperature required for the Stefan equation has not been the focus of calculation for atmospheric models. Ground surface temperatures are not normally measured at standard meteorological stations and thus are not readily available for use in hydrological or permafrost models.

Similar challenges in calculating soil temperature from limited available information have been addressed in biological studies (Bocock *et al*., 1977) because soil temperature is important to nutrient, soil respiration, carbon exchange and other biological processes. Several techniques have been used to relate air temperature to soil temperature such as harmonic analysis (Brown *et al*., 2000), time lags and autocorrelations (Gehrig-Fasel *et al*., 2008), and running averages (Zheng *et al*., 1993). Additionally, multiple regressions have been developed for calculating soil temperature using a range of variables including solar radiation, precipitation and leaf area index (Bocock *et al*., 1977; Zheng *et al*., 1993; Rankinen *et al*., 2004). While these studies were each successful in developing simplified relationships for calculating soil temperature, their widespread application is limited by the scope or location of the study as they require calibration at the site level.

In hydrological studies, ground surface temperatures are commonly expressed using the ratio of surface to air temperature (typically measured at 1.5 m height) known as the *n*-factor (n_t). *n*-factors have been used to improve the calculation of thaw depths using the Stefan equation (Klene *et al*., 2001); however, they are site-specific and vary depending on soil properties (Karunaratne and Burn, 2004), land cover type (Klene *et al*., 2001; Lewkowicz *et al*., 2012), local climate conditions and exposure to solar radiation (Juliussen and Humlum, 2007). Measurements from 13 locations within the Wolf Creek Research Basin near Whitehorse, Yukon, Canada, found n_t values ranging from 0.80 to 1.08 (Roadhouse, 2010). Studies from the Alaskan North Slope, USA (Klene *et al*., 2001), the Mackenzie valley between Fort Simpson and Norman Wells, Northwest Territories, Canada (Taylor, 1995), central Yukon (Karunaratne and Burn, 2004) and Northern Norway (Gisnås *et al*., 2013) also found high regional and small-scale variations, with n_t ranging from 0.3 to 1.4. Attempts have been made to categorize n_t on a regional basis (Juliussen and Humlum, 2007; Lewkowicz *et al*., 2012; Gisnås *et al*., 2013) based on vegetation classes and potential incoming radiation; however, without a universally applicable model, *n*-factors remain difficult to apply without site calibration.

A challenge with the *n*-factor approach is that it varies over the thaw season. Karunaratne and Burn (2004) calculated 10-day n_t values and showed that these values continued to increase early in the thaw season until the thaw progressed to a depth beyond diurnal temperature variations, at which time n_t became steady with a value near 1. Roadhouse (2010) noted similar seasonal variation patterns within Wolf Creek. To address this issue in ground thaw calculations, Woo *et al*. (2007) applied a simple empirical relationship that allowed the surface–air temperature ratio to vary as a function of time following the onset of ground thaw. Such an approach is necessary because when only a seasonal n_t is applied, there is the potential for problems simulating active layer thaw early in the thaw season when it is critical for hydrological calculations of subsurface water storage and flow. Errors early in the thaw season will also propagate throughout the summer. As a result, a method for calculating ground surface temperature is required that is transferable between various cold region environments and capable of being applied in areas where minimal site-specific information is available.

The purpose of this study is to address the need for a simple and widely applicable method for calculating ground surface temperature in cold regions, which will be accomplished by developing an algorithm that (1) represents the radiative, conductive and convective (RCC) components of energy transfer; (2) is capable of coupling with a modified Stefan equation in order to simulate ground thaw; (3) is driven by data that can be readily obtained or easily calculated; and (4) is transferable among cold region environments without site calibration.

The new method for calculating ground surface temperature is intended to be incorporated into the cold regions hydrological model (CRHM), a modular modelling platform for hydrological simulation in which the user selects the desired processes and basin structure to be represented (Pomeroy *et al*., 2007). CRHM includes a 'soil' module that is divided into three subsurface layers and is discussed in great detail by Fang *et al*. (2013). Current model applications have identified deficiencies in estimating runoff in the post-snowmelt period because of overestimation of available subsurface storage and underestimation of hydraulic conductivity, both of which appear to change with time (Carey and DeBeer, 2008). By incorporating a thaw depth calculation using a Stefan equation driven with ground surface temperatures and restricting the ability of water to flow beneath such a depth, it is anticipated that CRHM performance in estimating runoff generation will improve (Fang *et al*., 2013; Rasouli *et al*., 2014).

METHODOLOGY

Study sites

Data from three hydrological research basins in Western Canada are used in this study (Figure 1): Wolf Creek, Scotty Creek (SC) and Marmot Creek. Each study basin consists of multiple climate stations occupying a range of land cover types as described in Table I.

Wolf Creek (60°31′N, 135°31′W) is a mountain basin near Whitehorse, Yukon, in the Boreal Cordillera Ecozone. Approximately 43% of the basin is underlain by permafrost (Lewkowicz and Ednie, 2004), predominately at higher elevations and beneath north-facing slopes. The basin has three land cover types that are primarily determined by elevation. The lower basin (below 1100 m) is boreal forest, the upper (above 1500 m) is alpine tundra and the mid elevation is subalpine taiga with substantial shrub coverage. Each land cover type is represented by a long-term comprehensive meteorological station: Forest (750 m), Alpine (1615 m) and Buckbrush (1250 m), which have been operating since 1993. Additionally, several sites have been monitored for shorter time periods within Granger Basin, a subalpine to alpine tributary of Wolf Creek (Table I).

Scotty Creek (SC, 61°18′N, 121°18′W) is a discontinuous permafrost peatland located 50 km south of Fort Simpson, Northwest Territories in the Taiga Plains Ecozone. The terrain is level except where the presence of permafrost gives rise to plateaus that extend 1–2 m above the surrounding wetlands and produce an open black spruce canopy. The surrounding fens and bogs are saturated and generally do not support trees. Two meteorological stations represent differing land types: a bog in the permafrost-free wetland and a plateau beneath a sparse black spruce canopy.

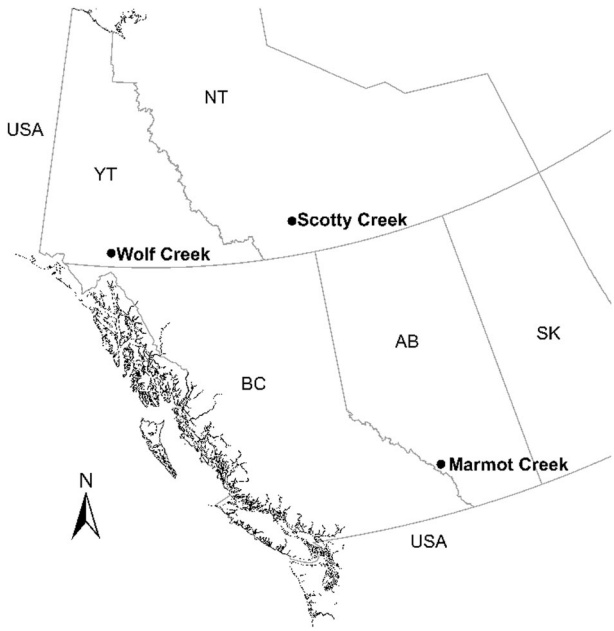

Figure 1. Map of Western Canada depicting the location of the three study sites used to test the RCC approach

Marmot Creek (50°57′N, 115°10′W) is a small headwaters drainage in the Canadian Rockies near Kananaskis, Alberta, on the eastern edge of the Montane Cordillera Ecozone. The basin is characterized by dramatic internal variation with steep north-facing and south-facing slopes and generally increasing precipitation and decreasing temperature with elevation that ranges from 1585 to 2805 m. Deep snowpacks and cool spring temperatures at high elevations result in snowcover in the alpine and treeline zones persisting well into July. At high elevations, there is discontinuous alpine permafrost. Two meteorological stations from Marmot are used for analysis: Level Forest (a low-elevation mature lodgepole forest) and Fisera Ridge (a high-elevation exposed alpine tundra ridge).

n-Factor thaw calculations

The modified Stefan equation used to simulate active layer thaw takes the general form

$$z = \frac{2\,k\,86400\sum(T_s{*}1\ \text{day})^{0.5}}{pwL} \tag{1}$$

where z is the depth of the thawing front from the ground (m), k is the thermal conductivity ($\mathrm{W\,m^{-1}\,°C^{-1}}$), 86 400 is a unit conversion ($\mathrm{s\,day^{-1}}$), T_s is the daily mean ground surface temperature (°C), ρ is the density of ice ($\mathrm{kg\,m^3}$), ω is the volumetric ice fraction and L is the latent heat of fusion ($334\,000\,\mathrm{J\,kg^{-1}}$). Use of the standard Stefan equation is most appropriate in saturated and homogenous soils; however, several attempts have been made to improve the applicability of the equation (Woo *et al.*, 2004; Hayashi *et al.*, 2007). Such applications still require the ground surface temperature as a driving variable.

The ground surface temperature is affected by atmospheric, vegetation and soil properties that impact the turbulent and radiative heat transfers that make up the surface energy budget. Calculation of these processes to solve for ground surface temperature is a data-intensive process that is not viable in areas where site or meteorological information is limited, and so, the approach that has been used in engineering and permafrost research is to relate the ground surface temperature to air temperature using an n-factor (Lunardini, 1978; Klene *et al.*, 2001). The n-factor is

Table I. Description of the ten climate stations used in the study from Wolf Creek (WC), Scotty Creek (SC) and Marmot Creek (MC) research basins

Site	Elevation (m)	Terrain	Vegetation	Organic Thickness (cm)	Surficial Material	Ground Thermal	Instrumentation			RCC Development
							Air Temp.	Net Radiation	Soil Temp.	
WC Forest	750	Valley bottom	15-18m white spruce (*Picea glauca*)	10–15	Silt loam	Seasonal frozen	HMP35	Delta-T	YSI 40328 (5, 15, 30, 80cm)	1999, 2000
WC Alpine	1615	Hilltop	Lichen, moss, bare	<4	Coarse till	Probable deep Permafrost	HMP35	NR-Lite	YSI 40328 (5, 15cm)	1997, 1998
WC Buckbrush	1250	Lower slope	1–3m willow shrub (*Salix*)	6	Alluvial silt	Seasonal frozen	HMP35	NR-Lite	YSI 40328 (5, 15, 30, 80cm)	n/a
WC Granger 3	1451	South-facing moderate slope	<1m dwarf birch (*betula glandulosa*)	2	Sandy till	Seasonal frozen	HMP35	REBS	Type E TC (5, 15cm)	2001, 2002
WC Granger 4	1490	North-facing moderate slope	<1m willow shrub (*Salix*)	20–24	Sandy till	Permafrost	HMP35	REBS	Campbell 107B (2, 5, 7.5, 10, 15, 20, 25, 30, 35, 40cm)	n/a
WC Granger 2	1411	Valley bottom	1–1.5m willow shrub (*Salix*)	8–10	Alluvial silt	Seasonal frozen	HMP35	n/a	Type E TC (5, 15cm)	n/a
SC Plateau	269	Plain	Black spruce (*Picea mariana*)	300–400	Glaciofluvial clay and silt	Permafrost	HMP45	CNR1	Campbell 107B (0, 5, 10, 15, 20, 25, 30, 40, 50, 60,70cm)	n/a
SC Bog	269	Plain	moss (*Sphagnum sp.*)	300-400	Glaciofluvial clay and silt	Seasonal frozen	HMP45	CNR1	Campbell 107B (10, 20, 30, 40, 50, 60, 80, 100cm)	n/a
MC Level Forest	1557	Lower slope	Lodgepole pine (*Pinus contorta*)	10	Silt loam over clay loam	Seasonal frozen	HMP45	CNR1	Campbell 107B (5, 25, 40cm)	n/a
MC Fisera Ridge	2325	Ridge top	grass, bare	2	Loam	Seasonal frozen	HMP45	CNR1	Campbell 107B (5, 15cm)	n/a

MC soil information is obtained from Beke (1969). HMP35, Vaisala HMP35CF hygrothermometer; HMP45, Vaisala HMP45C212 hygrothermometer; Delta-T, Delta-T 1m tube; NR-Lite, Kipp and Zonen NR-Lite net radiometer; REBS, REBS Q*7.1 net radiometer; CNR1, Kipp and Zonen CNR1 Pyranometer, Pyrgeometer.

defined as a seasonal value such that during the thaw season,

$$n_t = \frac{TDD_s}{TDD_a} \approx \frac{\sum \overline{T}_s}{\sum \overline{T}_a} \tag{2}$$

where TDD_s and TDD_a are the ground surface and air temperature thaw degree days, and $\overline{T}_s$ and $\overline{T}_a$ are the daily mean surface and air temperatures during the thaw season. Thus, an *n*-factor of 1 indicates the ground surface temperature is equal to the air temperature.

An uncertainty analysis associated with the use of an *n*-factor in Wolf Creek is performed using a regional study of *n*-factors in the southern Yukon (Lewkowicz *et al.*, 2012) that provides a range of values for each of the three primary land cover types found in Wolf Creek (Table II). The range of *n*-factors was then used to drive a simple two-layer (organic above mineral) Stefan equation following the method of Hayashi *et al.* (2007), where observed air temperatures and soil moisture percentages were measured from four thaw seasons (2001, 2007, 2008 and 2011) at the three long-term Wolf Creek monitoring stations. Multiple simulations were run for each land cover type using a range of organic layer thickness as observed from soil surveys and a range of soil properties (Table II) as measured from Wolf Creek geophysical studies (Seguin *et al.*, 1998). For each set of soil conditions, the uncertainty was expressed as a difference in maximum thaw depth between the upper and lower ranges of tested *n*-factors (Table II). Thaw calculations for the range of *n*-factors were performed on 48 combinations of organic thickness, porosity and ice contents per year, for a total of 192 uncertainty calculations per land type.

Development of the radiative–conductive–convective algorithm

Ground surface temperature is a function of the energy balance at the air-surface interface based on the fluxes of net radiation (radiative), ground heat (conductive), and sensible and latent heat (convective). Despite the assumptions behind many land surface schemes, a common reference temperature for all of these fluxes rarely exists (Pomeroy *et al.*, 2009; Bewley *et al.*, 2010). The development and operation of multiple source, resistance networks land surface models appropriate for cold regions environment remains prone to error because of high parameter and driving variable demand (Ménard *et al.*, 2014) such that they have only been applied experimentally at well-instrumented sites. As such, a physically guided approach based on an empirical assessment of three variables that represent the primary features of the ground surface energy balance is proposed here. The three variables are the sub-canopy net radiation, the daily mean air temperature (index of the sensible and latent fluxes) and the previous day frost table position (index of the ground heat flux). This approach assumes that variations in ventilation, due to wind speed variability, and evaporative cooling, due to humidity gradient variability, are small.

In the RCC approach, air temperature and net radiation are related to ground surface temperature using a simple linear relationship that is multiplied by a factor ranging between 0 and 1 depending on the frost table position

$$T_S = [aT_a + bR_n]\, m \tag{3}$$

where m is the frost table multiplier, expressed with a tangent function such that

$$m = \tan^{-1}(c(FT + d))/90 \tag{4}$$

By combining (3) and (4), the general form of the RCC algorithm is

$$T_s = [aT_a + bR_n] \cdot \left[\tan^{-1}(c\,(FT + d))/90\right] \tag{5}$$

where T_s and T_a are the daily mean ground surface and air temperatures (°C), R_n is the daily mean net radiation beneath the canopy (Wm^{-2}), FT is the previous day frost table depth (m), and a, b, c and d are the coefficients. The tangent function was chosen because saturated frozen ground conditions close to the ground surface produces a

Table II. Range of parameters applied to the *n*-factor uncertainty analysis in Wolf Creek

Parameters	Data source	Boreal forest	Subalpine taiga	Alpine tundra
n-Factor	Lewkowicz *et al.*, 2012	0.59–1.02	0.67–1.2	0.95–1.09
Organic thickness	Yukon Environment	0–23 cm	1–38 cm	0–4 cm
Porosity	Seguin *et al.*, 1998	21–65%	27–46%	23–36%
Ice content	Seguin *et al.*, 1998	13–21%	13–24%	12–28%

Organic thickness is from soil surveys conducted within the basin by Yukon Environment ($n = 15$ for forest, 33 for shrub-tundra subalpine taiga and 12 for alpine). Porosity and ice content are from geophysical surveys.

high thermal conductivity and a steep temperature gradient, resulting in a large ground heat flux and relatively lower surface temperature. As the frost table descends, its impact on the ground surface temperature diminishes. With a deep frost table position or complete soil thaw, the tangent function will approach 1, and the surface temperature becomes a function of only the air temperature and net radiation.

The RCC algorithm was developed during the thaw season using meteorological data collected from each of the three primary land cover types (forest, subalpine taiga and alpine tundra) in the mountainous subarctic Wolf Creek Research Basin (Table I). The thaw season is assumed to begin when the ground becomes snow-free as determined from albedo and snow depth measurements at each site. Air temperature, net radiation and ground surface temperature (5 cm depth) were measured directly at each site, and frost table depth was determined by the passage of the zero-degree isotherm interpolated linearly between the array of soil thermistors (Table I). Net radiation was measured beneath the canopy at the forest site, and above the shrubs at the subalpine stations. Two years of complete data coverage was selected for each site.

Equation (3) can be rewritten in a form where coefficients a and b can be solved using a multiple linear regression with a zero intercept

$$T_s = a(mT_a) + b(mR_n) \tag{6}$$

In order to perform the regression, frost table coefficients c and d must be chosen for Equation (4). The value of d must be a small positive value in order to avoid a multiplier that approaches zero that would prevent the onset of ground thaw. Several combinations of these coefficients were tested on a trial-and-error basis and determined to provide the best results with $c = 7$ and $d = 0.03$. Using these as an input to solve for coefficients a and b, the best fit multiple linear regression to the RCC algorithm is

$$T_s = [0.77T_a + 0.02R_n] \cdot \left[\tan^{-1}(7(FT + 0.03))/90\right] \tag{7}$$

The residual mean squared error was 2.6, and the predicted values compared well with the observed over the entire range of data for all three sites.

Figure 2 illustrates the relative importance of the three predictor variables in Equation (7). When the frost table is close to the ground surface, it is the dominant control on the calculation of the ground surface temperature. According to the best fit RCC algorithm, at a frost table depth of 5 cm, a 1 °C change in T_a induces a 0.25 °C change in the calculated T_s, while a 15-Wm^{-2} increase in R_n induces an increase of just 0.1 °C. As the frost table depth increases, small changes in the frost table depth become inconsequential for determining ground surface temperature. At these greater thaw depths, the multiplier approaches zero, and air temperature becomes the dominant control with a 1 °C change in T_a inducing a nearly 0.77 °C increase in calculated T_s, while a 15-Wm^{-2} increase in R_n induces a nearly 0.3 °C change in the calculated T_s (Figure 2).

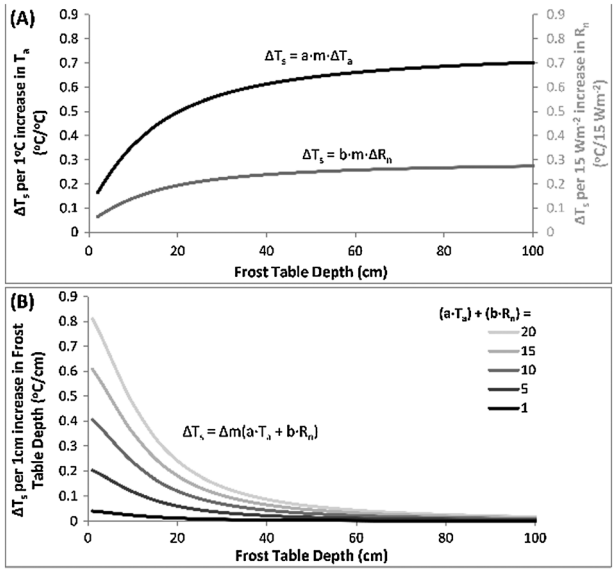

Figure 2. Sensitivity of variables in the RCC relation (with $a = 0.77$, $b = 0.02$) to (A) changes in air temperature and net radiation and (B) changes in frost table depth. In each case, the change in calculated ground surface temperature is based on the position of the frost table (x-axis)

Radiative–conductive–convective validation

The RCC algorithm was tested against observed data from five Wolf Creek stations, using different years of data for the three sites that were also involved in the calibration process. Additionally, the approach was tested on four climate stations outside of Wolf Creek, using data from the Marmot Creek and SC research basins (Table I). Calculated ground surface temperatures were compared with observations at each site, and the differences were expressed as a mean absolute error (MAE) and a root mean squared error.

Lastly, the RCC algorithm was coupled with a modified form of the Stefan equation, as described by Hayashi *et al.* (2007), at two sites that both contain permafrost and are well instrumented: the north-facing slope of Granger Basin (GB4) and the SC Plateau. At both sites, observed air temperature and net radiation were used to drive the RCC algorithm, and soil moisture measurements were used to calculate the bulk thermal conductivity (de Vries, 1963) based on a solid conductivity of $0.21\,Wm^{-1}K^{-1}$ for peat and

2.5 $Wm^{-1}K^{-1}$ for mineral soil. The porosity of the organic material was measured from soil samples at each site (0.90 to 0.98 at GB4 and 0.82 to 0.92 at SC Plateau) and estimated for the GB4 mineral layer based on the saturated soil moisture content of the 40-cm sensor (0.35).

Results of the coupled RCC thaw calculations were compared with those calculated from observed ground surface temperatures measured within 2 cm of the surface, as well as range of possible *n*-factors for each region (Taylor, 1995; Lewkowicz *et al.*, 2012). All thaw calculations were initiated upon the onset of snow-free conditions.

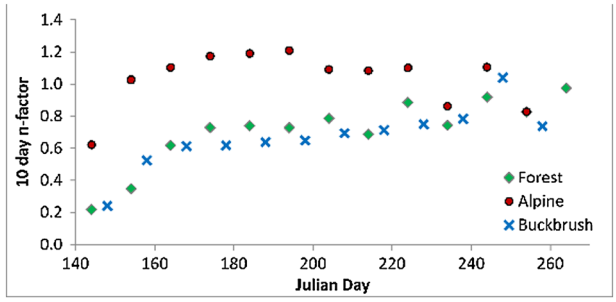

Figure 3. *n*-Factors expressed over 10-day period during the 2007 thaw season at three Wolf Creek sites. The low values of n_t early in the thaw season is a typical pattern caused by the presence of frozen soil close to the ground surface

RESULTS

Wolf creek n-factor

Thaw season *n*-factors for six Wolf Creek meteorological stations are shown in Table III. As observed in previous studies, there was considerable temporal and spatial variation in thawing *n*-factors for Wolf Creek. Higher *n*-factors were measured at the sparsely vegetated Alpine station (mean 0.99) and the southerly exposed subalpine station at Granger 3 (1.16), while lower *n*-factors were measured at the Forest (0.73) and Buckbrush (0.69).

By dividing the thawing season into 10-day increments and calculating an *n*-factor for each period, Figure 3 illustrates a pattern of variability within the thaw season that is typical of the Wolf Creek sites.

Table III. Thaw season *n*-factors observed at Wolf Creek

	Buckbrush	Alpine	Forest	Granger 2	Granger 3	Granger 4
Year						
1997		0.97	0.71			
1998	0.71	0.93	0.71			
1999	0.73		0.73	0.68	1.08	
2000			0.78	0.69	1.21	
2001	0.85	1.03	0.77	0.71	1.16	
2002		0.98			1.20	0.65
2003			0.74		1.15	
2004			0.72			
2005	0.76	0.99				
2006	0.67	1.00				
2007	0.67	1.04	0.73			
2008	0.61	1.03	0.71			
2009	0.62	0.91				
2010	0.65	0.96				
2011	0.75	1.02	0.78			
2012	0.61	1.02	0.71			
2013	0.62	0.99				
2014		1.00	0.69			
Std. dev.	0.07	0.04	0.03			
Mean	0.69	0.99	0.73	0.69	1.16	0.65

The Forest and Buckbrush sites had *n*-factors between 0.22 and 0.24 at the start of the thaw season, rising to 0.62 by days 20 to 30, and steadily approaching 1 by the end of the summer. The Alpine site was more consistent throughout the thaw season, but as with the other sites, it had a substantially lower *n*-factor of about 0.62 during the first 10 days of the thaw season.

In addition to the *n*-factor variation among sites and within a thaw season, the long-term monitoring stations also showed inter-annual variation. Thaw season *n*-factor variation was greatest at the Buckbrush station (0.61 to 0.76 with outlier of 0.85), compared with the Alpine station (0.93 to 1.04) and the Forest (0.69 to 0.78). The three sources of thaw season *n*-factor variation (spatial, inter-annual and intra-seasonal) illustrate the difficulty in choosing a single value to apply for the purposes of calculating ground thaw.

The potential range of *n*-factors for each of the Wolf Creek land cover types induced a high degree of uncertainty for calculating ground surface temperature and thus the frost table depth. Thawing season *n*-factors at the six Wolf Creek stations (Table III) generally fell within the expected range for their given land cover type (Table II), with the exception of the subalpine stations Granger 4 and Buckbrush that occasionally fell slightly below the lower range of 0.69 suggested in the literature (Lewkowicz *et al.*, 2012). Based on the potential range of *n*-factors in the literature for each of the Wolf Creek land cover types, the upper and lower ranges produced uncertainties in calculating ground surface temperature of 53% (boreal forest), 57% (subalpine taiga) and 14% (alpine tundra). By applying the range of *n*-factors in Stefan equations for a variety of soil conditions, end-of-season median uncertainty in frost table position was 0.66 m (30%) for boreal forest, 0.62 m (33%) for subalpine taiga and 0.19 m (7%) for the alpine tundra (Figure 4).

The uncertainty analysis suggests that the lowest and least variable uncertainty in the *n*-factor is associated with the alpine land cover because of its lack of vegetation and consistent soil properties. This leads to a narrow range of

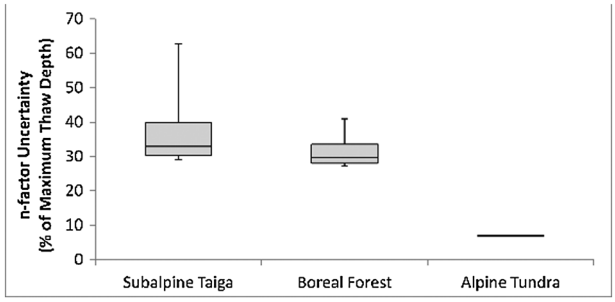

Figure 4. Boxplots depicting the minimum, maximum, median and quartiles for *n*-factor uncertainty calculated for each land cover type in Wolf Creek based on a range of possible soil properties and years of data input. The *n*-factor uncertainty is defined as the differences between the end-of-season thaw depth calculated for a range of potential *n*-factors

potential *n*-factors, which reduces the overall uncertainty of the frost table calculation. The range of uncertainty shown in Figure 4 was greatly reduced for the alpine due largely to the consistently thin organic layer. Thicker organic layers at lower elevations in Wolf Creek produced greater uncertainty in the simple two-layer thaw calculations because of the increased rate of thaw in the mineral layer. As shown for the thaw calculations for the boreal forest and subalpine land covers, uncertainty in the ground surface temperature induced uncertainty in the thaw calculation that is in large part dependent on site conditions such as the organic layer thickness, soil moisture and ice content.

Radiative–conductive–convective validation

Application of the RCC algorithm at all five Wolf Creek sites produced good results in replicating the observed ground surface temperatures (Figure 5), with the exception of Buckbrush (MAE = 2.3 °C) where calculated temperatures exceeded the observed values. At the other sites, the calculated mean thaw season ground surface temperature was within ±1 °C of the observed values, with an MAE < 2.0 °C. On occasion, the range of temperature was overestimated by the RCC algorithm; however, this is to be expected given that ground surface temperatures for these sites are 5 cm deep rather than at the surface. The true ground surface temperature has greater variability than the observed values, but the rapid damping of these temperatures beneath the ground surface means that this does not influence the rate of ground thaw.

The summary statistics in Figure 5 demonstrate the contribution of each driving variable of the RCC algorithm to represent different energy regimes. In the thaw seasons examined, the Alpine site had an average air temperature 5.1 °C below the Forest site; however, the effect on the calculated ground surface temperature was moderated by the increase in net radiation at the Alpine (average 109 Wm^{-2} greater than that of Forest). Similarly, comparison of Grangers 3 and 4 (south facing *vs* north facing) shows that the thaw season mean air temperature

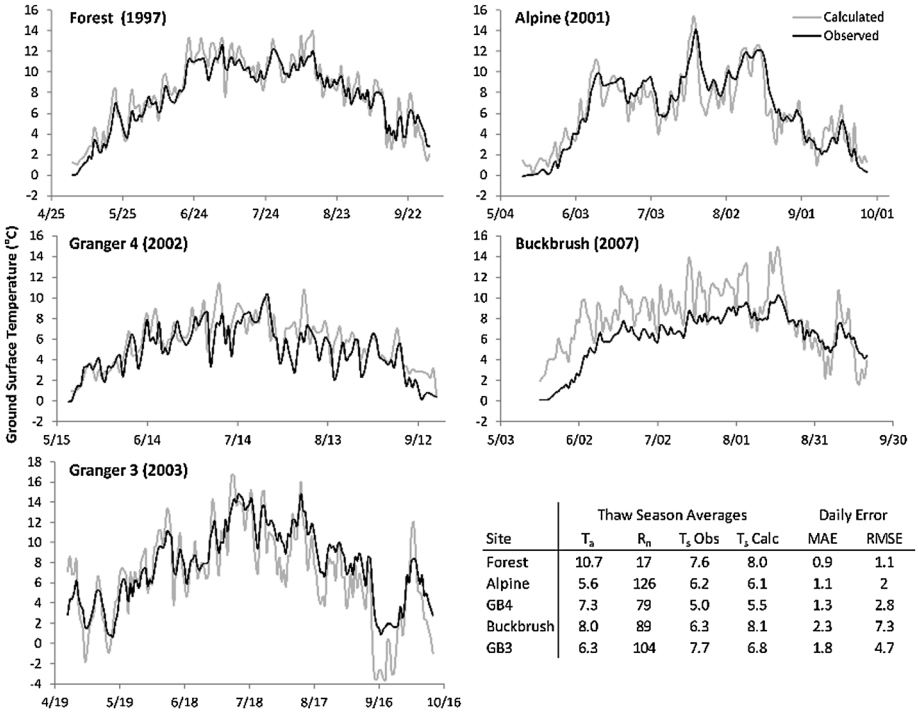

	Thaw Season Averages				Daily Error	
Site	T_a	R_n	T_s Obs	T_s Calc	MAE	RMSE
Forest	10.7	17	7.6	8.0	0.9	1.1
Alpine	5.6	126	6.2	6.1	1.1	2
GB4	7.3	79	5.0	5.5	1.3	2.8
Buckbrush	8.0	89	6.3	8.1	2.3	7.3
GB3	6.3	104	7.7	6.8	1.8	4.7

Figure 5. Ground surface temperatures during the thaw season calculated using the RCC approach (grey, T_s Calc) compared with observed values (black, T_s Obs) at five Wolf Creek sites. Thaw season averages and errors are summarized for each site where T_a is the mean air temperature and R_n is the mean net radiation over the thaw season

is slightly warmer for the Granger 4 site, but the calculated and observed ground surface temperatures are both warmer for Granger 3 because of the higher net radiation and the correspondingly faster ground thaw. The best performance of the RCC algorithm at both Grangers 3 and 4 was early in thaw season (Figure 5).

The RCC algorithm produced similarly good results when applied to a range of other cold region environments for which the model was not developed (Figure 6). Thaw season MAE between observed and calculated ground surface temperatures for these sites ranges from 1.3 to 2.4 °C. However, as with the Wolf Creek sites, the RCC algorithm performed better relative to observed values early in the thaw season with MAE ranging from 0.8 to 2.1 °C over the first 30 days of thaw. In particular, the algorithm underestimated ground surface temperature at the SC Bog beginning in mid-June, resulting in an average thaw season temperature that was 1.7 °C below the measured average.

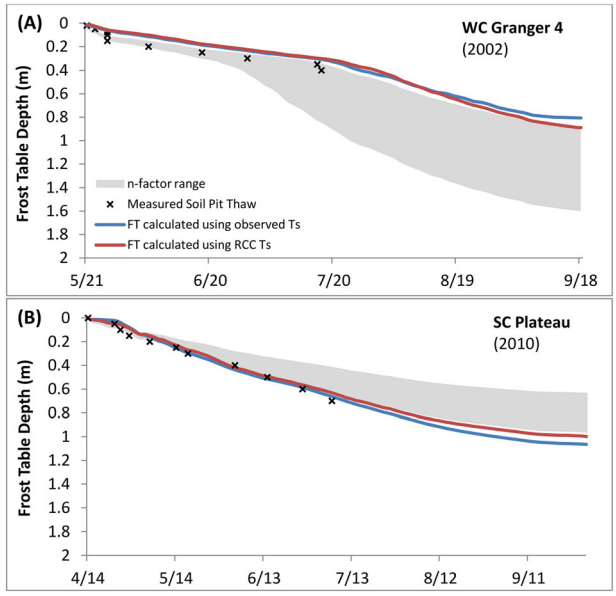

Figure 7. Frost table simulations for the north-facing slope in Granger Basin (GB4) and Scotty Creek Plateau using a modified Stefan equation driven with observed (blue) and RCC calculated (red) ground surface temperatures. The shaded region represents the progression of the thawing front using a range of possible *n*-factors, and the point thaw data correspond to the progression of the zero-degree isotherm as measured by a series of thermistors at each site

Ground thaw simulation

Figure 7 shows results of the coupled RCC–Stefan equation ground thaw calculations relative to Stefan equation thaw calculations driven by observed ground surface temperatures. The RCC approach performed very well in driving the Stefan equation, with end-of-season thaw depths at both sites within 10% of those driven by observed ground surface temperatures. At both sites, the differences in RCC calculated and observed ground surface temperatures mostly occurred later in the thaw season when they were not liable to propagate, resulting in only small differences in the calculated frost table depths. By the end of the thaw season, the RCC-driven

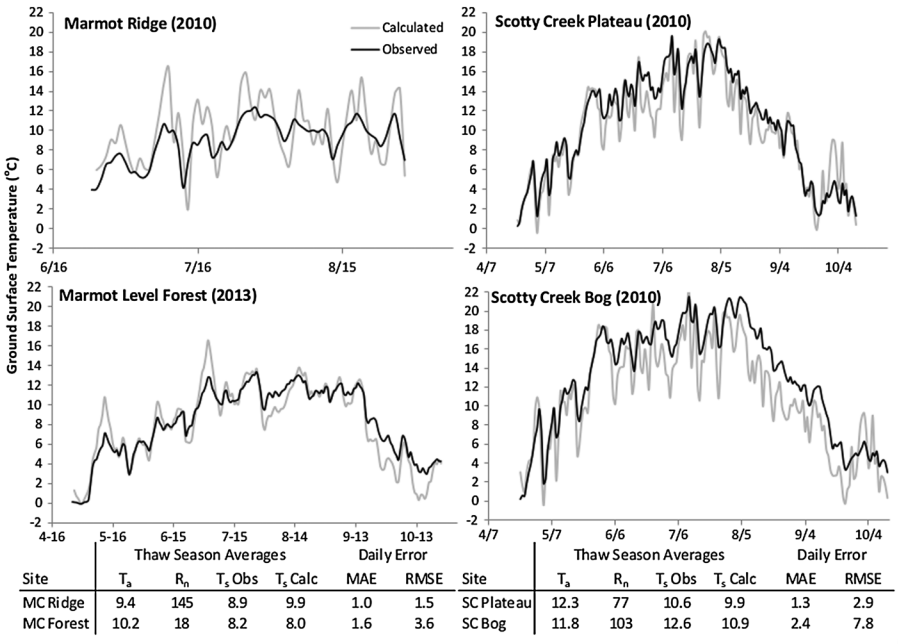

	Thaw Season Averages				Daily Error	
Site	T_a	R_n	T_s Obs	T_s Calc	MAE	RMSE
MC Ridge	9.4	145	8.9	9.9	1.0	1.5
MC Forest	10.2	18	8.2	8.0	1.6	3.6
SC Plateau	12.3	77	10.6	9.9	1.3	2.9
SC Bog	11.8	103	12.6	10.9	2.4	7.8

Figure 6. Ground surface temperatures during the thaw season calculated using the RCC approach (grey, T_s Calc) compared with observed values (black, T_s Obs) at two sites from Marmot Creek, AB, and two sites from Scotty Creek, NT. Thaw season averages and errors are summarized for each site where T_a is the mean air temperature and R_n is the mean net radiation over the thaw season

frost table was 8 cm deeper than that driven by observed ground surface temperatures at GB4, and 7 cm shallower at SC Plateau.

A range of *n*-factors was applied to the Stefan equation frost table calculations at both sites based on regional *n*-factor studies. For the subalpine site in the Yukon (GB4), a range of 0.67 to 1.2 was applied based on Lewkowicz *et al*. (2012), and for the forested site in the Mackenzie Valley (SC Plateau), a range of 0.3 to 0.7 from Taylor (1995) was applied. Neither of the two sites was used in the RCC development process; however, the difference between RCC and measured ground surface temperature-driven frost table depth calculations was substantially less than the uncertainty associated with the range of possible *n*-factors (Figure 7). For the early portion of the thaw season at GB4, the entire range of *n*-factors overestimated ground thaw because of the pattern of seasonal variation in *n*-factors (Figure 3).

DISCUSSION

The generalized RCC algorithm performed well when compared with observed ground surface temperatures at a variety of sites. It is a promising method for calculating ground surface temperatures that can be coupled with a Stefan-based algorithm to predict the depth of the frost table during soil thawing with limited site information requirements. The RCC method eliminates the need for site calibration that is necessary for the *n*-factor approach because of the high degree of uncertainty associated with applying unknown *n*-factors. While the *n*-factor remains a useful tool to calculate the end-of-season thaw depth for well-studied sites where it can be calibrated, it is not suitable for seasonal calculations of thaw over a drainage basin because of the importance of early spring frost table position and the need to spatially distribute calculations to a wide variety of land covers and terrain.

The inter-annual variation that occurs in the observed *n*-factor demonstrates the inability of the *n*-factor approach to represent inter-annual variation in climate. Several investigators have noted that soil surface temperatures will exhibit a nonlinear response to air temperature with climate change and that assumptions of future soil temperatures should not be based solely on air temperature (Mellander *et al*., 2007; Kurylyk *et al*., 2013; Jungqvist *et al*., 2014). The RCC method has the potential to be more robust than the *n*-factor approach in regard to warmer climates as it has the ability to represent changing radiation and soil thermal regimes.

The declining performance of the RCC algorithm for calculating ground surface temperature later in the summer season is most likely due to cumulative errors in calculating the frost table position over several months and neglect of subsurface heat storage in the algorithm. In many sites, this is not important; for instance, SC Bog is a wetland with a very high heat capacity that results in relatively warm ground surface temperatures late in the summer; however, frozen ground at this site only persists for 1 to 2 weeks into the thaw season. As such, the poorer RCC performance late in the summer is irrelevant.

It should be noted that thaw calculations performed in this study were performed using a simple method that was intended for thick organic soils (Hayashi *et al*., 2007). The intent of the paper was to develop an equation for calculating ground surface temperature and not to test a particular thaw equation. The RCC approach is designed to be used with a variety of thaw algorithms, examples of which are discussed by Kurylyk and Watanabe (2013) and Zhang *et al*. (2008). Given the promising results of this study, future work will couple the RCC equation with a thaw algorithm and a method for calculating surface temperature beneath snow using the lower layer snow temperature from models such as SNOBAL (Marks *et al*., 1999) that is a module in CRHM that produces useful lower snowpack temperatures (DeBeer and Pomeroy, 2009). This will assess the potential for the RCC approach to represent thaw processes over multiple years and model permafrost response of which would be useful to hydrological and permafrost engineering applications.

The one site that was not well simulated by the RCC approach at any time during the thaw season was the Buckbrush site at Wolf Creek in which the observed ground surface temperature was overestimated. This is likely due to using above-canopy air temperatures and net radiation to drive what is more appropriately a sub-canopy calculation. Sub-canopy radiation and temperature have been estimated for snowmelt periods using dual-source resistance models (Bewley *et al*., 2010) in these environments and have been found to be substantially different from above-canopy conditions. It is recommended that the RCC method be used with sub-canopy radiation and temperature estimation where these exist.

The poor performance at the Buckbrush site may also be in part due to the uncertainty associated with small-scale variation in the parameters that drive the RCC approach. Soil conditions such as moisture content and ice fraction can vary considerably over short distances and result in variable soil surface temperatures. Net radiation can pose similar challenges because of subtle differences in exposure and vegetation, particularly in the case of discontinuous forest canopies where solar radiation can be highly variable even when integrated over daily time steps (Pomeroy *et al*., 2008). Generalization of ground surface temperature and frost table depths over land types will inevitably contain uncertainty associated with these small-scale variations.

The most notable disadvantage to the RCC approach is the net radiation data requirement. Use of net radiation allows for more accurate ground surface temperature calculations on sloped surfaces and beneath tree canopies; however, net radiation is not a variable that is commonly measured. Fortunately, net radiation can be easily estimated from incoming solar radiation estimates or from algorithms that rely on diurnal temperature variations to deduce atmospheric transmittance that can be used with clear sky solar irradiance calculations (Granger and Gray, 1990; Pomeroy *et al*., 2007; Shook and Pomeroy, 2011) to estimate net radiation above or below canopies or on slopes (Sicart *et al*., 2006; Ellis *et al*., 2010). These algorithms are implemented in CRHM and have been used for large area evapotranspiration calculations on decadal timescales using air temperature, cloudiness and humidity (Armstrong *et al*., 2015), and so, their application for soil thaw calculations is not technically challenging. Alternatively, detailed land surface schemes such as Canadian land surface scheme (Verseghy, 1991) or shrub-tundra canopy energetics models such as the dual-source or triple-source resistance schemes outlined by Bewley *et al*. (2010) and Ménard *et al*. (2014) can be used to drive the calculation.

In addition to the use of net radiation, the RCC algorithm also incorporates a frost table parameter that allowed for better representation of cold ground surface temperatures early in the thaw season. This inherently creates the possibility of feedback errors within the computation. When coupled with a modified Stefan equation, obtaining accurate ground surface temperature is dependent on the parameters set within the frost table calculation such as thermal conductivity and fraction of ice content. This is particularly important with the initial conditions prior to the onset of thaw, and so, when coupling the RCC algorithm with a Stefan equation, it is necessary to have sufficient resolution of soil layers such that near-surface conditions are accurately portrayed.

CONCLUSIONS

Use of the *n*-factor to calculate the frost table from air temperature is problematic for seasonal calculations needed in hydrology because of its spatial and temporal variability that necessitates site-specific calibration and limits its applicability early in the thaw season when the frost table position is the most important to runoff processes. The RCC algorithm developed here provides an alternative approach, which considers air temperature, surface net radiation and frost table position and so is sensitive to soil properties and recent meteorological and hydrological history at the site.

The RCC approach performed very well in calculating ground surface temperatures in a variety of land cover types in three cold region basins in Canada. The algorithm requires substantially less site information than a conventional energy balance approach as employed in detailed land surface or resistance network schemes to calculating ground surface temperature. This allows for application as part of evolving CRHMs in areas where site-specific driving meteorology and detailed canopy parameters are limited or uncertain. The algorithm performed well when coupled with a Stefan-based approach for simulating progression of the thawing front, demonstrating its potential to be incorporated into models that calculate frost table depth. Improved frost table simulations in such models is expected to result in better simulation of subsurface hydrological processes in cold regions dominated by frozen ground conditions.

ACKNOWLEDGEMENTS

The authors acknowledge funding from the Yukon Environment, the NSERC Changing Cold Regions Network, the CFCAS IP3 Network, and Alberta Environment and Sustainable Resource Development. We wish to thank the Liidlii Kue First Nation and Dehcho First Nations in Fort Simpson, and the Jean-Marie River First Nation for their support of field studies at Scotty Creek. We would like to thank the countless number of researchers and technicians who have maintained the long-term data records from these research basins, and Yukon Environment Fish and Wildlife Branch for providing soil survey data in Wolf Creek. The authors thank an anonymous reviewer and Barret Kurylyk for their insightful comments that led to an improved manuscript.

REFERENCES

Armstrong RN, Pomeroy JW, Martz LW. 2015. Variability in evaporation across the Canadian Prairie region during drought and non-drought periods. *Journal of Hydrology* **521**: 182–195.

Beke GJ. 1969. Soils of three experimental watersheds in Alberta and their hydrological significance – Ph.D. thesis. University of Alberta: Edmonton; 456.

Bewley D, Essery R, Pomeroy JW, Menard C. 2010. Measurements and modelling of snowmelt and turbulent heat fluxes over shrub tundra. *Hydrology and Earth System Science* **14**: 1331–1340.

Bocock KL, Jeffers JNR, Lindley DK, Adamson JK, Gill CA. 1977. Estimating woodland soil-temperature from air temperature and other climatic variables. *Agricultural Meteorology* **18**: 351–372.

Brown SE, Pregitzer KS, Reed DD, Burton AJ. 2000. Predicting daily mean soil temperature from daily mean air temperature in four northern hardwood forest stands. *Forest Science* **46**: 297–301.

Carey SK, DeBeer CM. 2008. Rainfall-runoff hydrograph characteristics in a discontinuous permafrost watershed and their relation to ground thaw. Proceedings, Ninth International Conference on Permafrost. University of Alaska Fairbanks; 233–238.

Carey SK, Woo M. 2005. Freezing of subarctic hillslopes, Wolf Creek Basin, Yukon, Canada. *Arctic, Antarctic, and Alpine Research* **37**: 1–10.

DeBeer CM, Pomeroy JW. 2009. Modelling snow melt and snowcover depletion in a small cirque, Canadian Rocky Mountains. *Hydrological Processes* **23**: 2384–2599.

Ellis CR, Pomeroy JW, Brown T, MacDonald J. 2010. Simulation of snow accumulation and melt in needleleaf forest environments. *Hydrology and Earth System Sciences* **14**: 925–940. DOI:10.5194/hess-14-925-2010.

Fang X, Pomeroy JW, Ellis CR, MacDonald MK, DeBeer CM, Brown T. 2013. Multi-variable evaluation of hydrological model predictions for a headwater basin in the Canadian Rocky Mountains. *Hydrology and Earth System Science* **9**: 12825–12877. DOI:10.5194/hessd-9-12825-2012.

Gehrig-Fasel J, Guisan A, Zimmermann NE. 2008. Evaluating thermal treeline indicators based on air and soil temperature using an air-to-soil temperature transfer model. *Ecological Modelling* **213**: 345–355. DOI:10.1016/j.ecolmodel.2008.01.003.

Gisnås K, Etzelmüller B, Farbrot H, Schuler TV, Westermann S. 2013. CryoGRID 1.0: permafrost distribution in Norway estimated by a spatial numerical model. *Permafrost and Periglacial Processes* **24**: 2–19. DOI:10.1002/ppp.1765.

Granger RJ, Gray DM. 1990. A net radiation model for calculating snowmelt in open environments. *Nordic Hydrology* **21**: 217–234.

Hayashi M, Quinton WL, Wright N, Goeller N. 2007. A simple heat-conduction method for simulating the frost-table depth in hydrological models. *Hydrological Processes* **21**: 2610–2622. DOI:10.1002/hyp.6792.

Juliussen H, Humlum O. 2007. Towards a TTOP ground temperature model for mountainous terrain in central-eastern Norway. *Permafrost and Periglacial Processes* **18**: 161–184. DOI:10.1002/ppp.586.

Jungqvist G, Oni SK, Teutschbein C, Futter MN. 2014. Effect of climate change on soil temperature in Swedish boreal forests. *PLoS ONE* **9**e93957: . DOI:10.1371/journal.pone.0093957.

Karunaratne KC, Burn CR. 2004. Relations between air and surface temperature in discontinuous permafrost terrain near Mayo, Yukon Territory. *Canadian Journal of Earth Sciences* **41**: 1437–1451. DOI:10.1139/E04-082.

Klene AE, Nelson FE, Shiklomanov NI, Hinkel KM. 2001. The N-factor in natural landscapes: variability of air and soil surface temperatures, Kuparuk River basin, Alaska, USA. *Arctic, Antarctic, and Alpine Research* **33**: 140–148.

Kurylyk BL, Watanabe K. 2013. Review: the mathematical representation of freezing and thawing processes in variably saturated, non-deformable soils. *Advances in Water Resources* **60**: 160–177. DOI:10.1016/j.advwatres.2013.07.016.

Kurylyk BL, Bourque CPA, MacQuarrie KTB. 2013. Potential surface temperature and shallow groundwater temperature response to climate change: an example from a small forested catchment in east-central New Brunswick (Canada). *Hydrology and Earth System Sciences* **17**: 2701–2716. DOI:10.5194/hess-17-2701-2013.

Lewkowicz AG, Ednie M. 2004. Probability mapping of mountain permafrost using the BTS method, Wolf Creek, Yukon Territory, Canada. *Permafrost Periglacial Processes* **15**: 67–80. DOI:10.1002/ppp.480.

Lewkowicz AG, Bonnaventure PP, Smith SL, Kuntz Z. 2012. Spatial and thermal characteristics of mountain permafrost, northwest Canada. *Physical Geography* **94**: 195–213. DOI:10.1111/j.1468-0459.2012.00462.x.

Lunardini VJ. 1978. Theory of n-factors and correlation of data. Third International Conference on Permafrost (Edmonton, Canada). Centre d'études nordiques, Université Laval, Québec; **1**: 40–46.

Marks D, Domingo J, Susong D, Link T, Garen D. 1999. A spatially distributed energy balance snowmelt model for application in mountain basins. *Hydrological Processes* **13**: 1935–1959.

Mellander P, Lofvenius MO, Laudon H. 2007. Climate change impacts on snow and soil temperature in boreal Scots pine stands. *Climatic Change* **85**: 179–193. DOI:10.1007/s10584-007-9254-3.

Ménard CB, Essery R, Pomeroy JW. 2014. Modelled sensitivity of the snow regime to topography, shrub fraction and shrub height. *Hydrology and Earth System Science* **18**: 2375–2392.

Pomeroy JW, Gray DM, Brown T, Hedstrom NR, Quinton WL, Granger RJ, Carey SK. 2007. The cold regions hydrological model, a platform for basing process representation and model structure on physical evidence. *Hydrological Processes* **21**: 2650–2667.

Pomeroy J, Rowlands A, Hardy J, Link T, Marks D, Essery R, Sicart JE, Ellis C. 2008. Spatial variability of shortwave irradiance for snowmelt in forests. *Journal of Hydrometeorology* **9**: 1482–1490.

Pomeroy JW, Marks D, Link T, Ellis C, Hardy J, Rowlands A, Granger R. 2009. The impact of coniferous forest temperature on incoming longwave radiation to melting snow. *Hydrological Processes* **23**: 2513–2525. DOI:10.1002/hyp.7325.

Quinton WL, Bemrose RK, Zhang Y, Carey SK. 2009. The influence of spatial variability in snowmelt and active layer thaw on hillslope drainage for an alpine tundra hillslope. *Hydrological Processes* **23**: 2628–2639. DOI:10.1002/hyp.7327.

Rankinen K, Karvonen T, Butterfield D. 2004. A simple model for predicting soil temperature in snow-covered and seasonally frozen soil: model description and testing. *Hydrology and Earth System Sciences* **8**: 706–716.

Rasouli K, Pomeroy JW, Janowicz JR, Carey SK, Williams TJ. 2014. Hydrological sensitivity of a northern mountain basin to climate change. *Hydrological Processes* **28**: 4191–4208. DOI:10.1002/hyp.10244.

Roadhouse EA. 2010. Air and ground surface temperature relations in a mountainous basin, Wolf Creek, Yukon Territory – MSc Thesis. University of Ottawa: Ottawa; 156.

Seguin M-K, Stein J, Nilo O, Jalbert C, Ding Y. 1998. *Hydrogeophysical Investigation of the Wolf Creek Watershed, Yukon Territory, Canada*. Institut national de la recherché scientifique: Sainte-Foy, Quebec; 54.

Shook KR, Pomeroy JW. 2011. Synthesis of incoming shortwave radiation for hydrological simulation. *Hydrology Research* **42**: 433–446. DOI:10.2166/nh.2011.074.

Sicart JE, Pomeroy JW, Essery RLH, Bewley D. 2006. Incoming longwave radiation to melting snow: observations, sensitivity and estimation in northern environments. *Hydrological Processes* **20**: 3697–3708. DOI:10.1002/hyp.6383.

Taylor AE. 1995. Field measurements of n-factors for natural forest areas, Mackenzie Valley, Northwest Territories. In *Interior Plaines and Arctic Canada – Current Research 1995-B*. Geological Survey of Canada: Ottawa, Ontario; 89–98.

Verseghy DL. 1991. CLASS – a Canadian land surface scheme for GCMs. *International Journal of Climatology* **11**: 111–133.

de Vries DA. 1963. Thermal properties of soil. In *Physics of Plant Environment*, van Dijk WR (eds). North Holland Publishing: Amsterdam; 210–235.

Woo M-k. 1986. Permafrost hydrology in North America. *Atmosphere-Ocean* **24**: 201–234.

Woo M-k, Arain MA, Mollinga M, Yi S. 2004. A two-directional freeze and thaw algorithm for hydrologic and land surface modeling. *Geophysical Research Letters* **31**:L12501. DOI:10.1029/2004GL019475.

Woo M-k, Mollinga M, Smith SL. 2007. Climate warming and active layer thaw in the boreal and tundra environments of the Mackenzie Valley. *Canadian Journal of Earth Sciences* **44**: 733–743.

Zhang Z, Kane DL, Hinzman LD. 2000. Development and application of a spatial-distributed Arctic hydrological and thermal process model. *Hydrological Processes* **14**: 1591–1611.

Zhang Y, Carey SK, Quinton WL. 2008. Evaluation of the algorithms and parameterizations for ground thawing and freezing simulation in permafrost regions. *Journal of Geophysical Research* **113**D17116. DOI:10.1029/2007JD009343.

Zheng D, Hunt R, Running SW. 1993. A daily soil temperature model based on air temperature and precipitation for continental applications. *Climate Research* **2**: 183–191.